Solvation dynamics inside confined systems

M.Sc. Research Thesis

By

Mohit Kumar

2103131012

DEPARTMENT OF CHEMISTRY

INDIAN INSTITUTE OF TECHNOLOGY, INDORE

MAY 2023

Solvation dynamics inside confined systems

A THESIS

Submitted in partial fulfilment of the requirements for the award of the degree of

Master of Science

By

Mohit Kumar

DEPARTMENT OF CHEMISTRY

INDIAN INSTITUTE OF TECHNOLOGY

INDORE

MAY 2023

INDIAN INSTITUTE OF TECHNOLOGY INDORE

CANDIDATE'S DECLARATION

I hereby certify that the work presented in the thesis SOLVATION DYNAMICS INSIDE CONFINED SYSTEMS which was submitted to the DEPARTMENT OF CHEMISTRY, Indian Institute of Technology Indore, is an authentic record of my own work completed during the time period from July 2022 to May 2023. This thesis is being submitted in partial fulfilment of the requirement for the award of the degree of MASTER OF SCIENCE, under the supervision of Prof. Tushar Kanti Mukherjee, Department of Chemistry, IIT Indore.

Mohit Kumar. 22/5/23

Signature of the student with the date

(MOHIT KUMAR)

This is to certify that the above statement made by the candidate is correct to the best of my/our knowledge.

22/5/23

Signature of the Supervisor with the date

Prof. Tushar Kanti Mukherjee

MOHIT KUMAR has successfully given her M.Sc. Oral Examination held on 17/05/23

22/5/23

Signature of the Supervisor with the date

Prof. Tushar Kanti Mukherjee

S. Selvakumar (Dr. Selvakumar) Acting DPGC

Convener, DPGC

Date: 22.05.2023

A Chakraborty

Signature of PSPC Member

Prof. Anjan Chakraborty

Date: 22/05/2023

Dipak Kumar Roy

Signature of PSPC Member

Dr. Dipak Kumar Roy

Date: 22.05.2023

ACKNOWLEDGEMENTS

I express my heartful gratitude to my supervisor Prof. Tushar Kanti Mukherjee for his guidance throughout my project work. His dedication and confidence have been inspirational. His motivation, enthusiasm, understanding have been always helpful in this journey.

I wish to express my gratitude to PSPC members Prof. Anjan Chakraborty and Dr. Deepak Kumar Roy for their important suggestions during my project work.

I extended my thanks to my lab mates and my classmates for supporting and understanding me throughout my work.

I would like to acknowledge SIC, IIT Indore for all instrumentation facilities.

I express my love and respect to my family for their support and incredible love.

I thank each person who helped me during this journey.

MOHIT KUMAR

Dedicated to

My Family….

ABSTRACT

In the present work, we have observed the formation of micelles using different surfactants like SDS, CTAB, and SDS. Micelles are formed when concentration exceeds the critical micelle concentration. The coumarin 480 dye was used as a solute probe to understand the behaviour of water molecules inside the stern layer of micelles. The blue shift observed in the PL spectra of coumarin 480 was due to its presence in the stern layer of micelles which restricts the motion of water molecules. Furthermore, the behaviour of solute probe coumarin 480 was studied when encapsulated inside the ATP/PDADMAC droplet. The electrostatic interactions between negatively charged ATP and positively charged PDADMAC results in the fabrication of ATP/PDADMAC coacervates. The presence of coumarin 480 dye inside the ATP coacervates was confirmed using CLSM.

Next, different hybrid coacervate droplets were fabricated to study their interior environment using solvation dynamics. Here, we utilized negatively charged carbon dots (CDs), quantum dots (QDs) with a counterpart positively charged polymer (PDADMAC) to obtain CD-embedded coacervates and QD-embedded coacervates. The fabrication of these droplets was confirmed using CLSM and FESEM imaging and further, we fabricate HSA condensate @AuNCs.

TABLE OF CONTENTS

LIST OF FIGURES

LIST OF SCHEMES

LIST OF TABLES

NOMENCLATURE

ACRONYMS

Chapter 1 : Introduction

1.1 Solvation dynamics

1.2 Micelles

1.3 Stern layer

1.4 Nucleotides

1.5 Nanoparticle

1.5.1 Types of Nanoparticle

1.6 Nanocluster

1.6.1 Gold Nanocluster

1.7 Polyelectrolytes or polymer

1.8 Coacervate droplets

1.8.1 Quantum dot droplets

1.8.2 Carbon dot droplets

Chapter 2 : Experimental section

2.1 Micelles

2.1.1 Materials

2.1.2 Preparation of micelles Assembly formation or assimilation

2.2 ATP/PDADMAC droplet

2.2.1 Materials

2.2.2 Preparation of ATP/PDADMAC coacervate droplet

2.2.3 Preparation of coumarin 480 loaded ATP/PDADMAC droplet

2.3 Quantum dot droplet

2.3.1 Materials

2.3.2 Preparation of quantum dot

2.3.3 Preparation of quantum dot droplet

2.4 Carbon dot droplet

2.4.1 Materials

2.4.2 Preparation of carbon dot

2.4.3 Preparation of carbon dot droplet

2.5 N,P-Carbon dot droplet

2.5.1 Materials

2.5.2 Preparation of N,P-Carbon dot

2.5.3 Preparation of N,P-Carbon dot droplet

2.6 Gold nanocluster

2.6.1 Materials

2.6.2 Preparation of HSA capped gold nanoclusters

2.6.3 Preparation of HSA condensates @ gold NCs

2.7 Instrumentation

Chapter 3 : Results and Discussions

Chapter 4 : Conclusion and future work

REFERENCES

LIST OF FIGURES

Figure 1. Structure of Micelle

Figure 2. Structure of Stern layer

Figure 3. Structure of Adenosine triphosphate (ATP)

Figure 4. Structure of PDADMAC

Figure 5. Diagram of TCSPC

Figure 6. Emission spectra of probe coumarin 480 in water, 3.5mM CTAB, 2mM TX-100, 32mM SDS

Figure 7. Emission spectra of probe coumarin 480 in water and 32mM SDS micelle

Figure 8. Decays of solute probe coumarin 480 in 32 mM SDS at range of wavelength 450-600 nm

Figure 9. Time resolved emission spectra of coumarin 4800 in SDS micelle at different times

Figure 10. TRES of coumarin 480 in SDS micelle

Figure 11. C(t) of coumarin 480 in 32 mM SDS

Figure 12. FE-SEM and Confocal image of ATP/PDADMAC droplet

Figure 13. Confocal images of coumarin 480 loaded ATP droplet

Figure 14. Absorption spectra of coumarin 480 loaded ATP/PDADMAC droplet

Figure 15. Emission spectra of coumarin 480 in water and ATP droplet

Figure 16. Emission spectra of coumarin 480 in ATP/PDADMAC droplet at different times

Figure 17. Decays of solute probe coumarin 480 in ATP/PDADMC droplet at range of wavelength 440-600 nm

Figure 18. Time resolved emission spectra of coumarin 480 in ATP/PDADMAC droplet

Figure 19. TRES of coumarin 480 in ATP/PDADMAC droplet

Figure 20. (A) Absorption spectra, (B) Fluorescence spectra of green quantum dots and green quantum droplets, and

(C) Confocal images (DIC, FL, and merge) of green quantum droplets

Figure 21. (A) Absorption spectra, (B) Fluorescence spectra of red quantum dots and green quantum droplets, and (C) Confocal images (DIC, FL, and merge) of red quantum droplets

Figure 23. Absorption spectra of (A) dialysed or purified N,P-Carbon dots, (B) crude N,P-Carbon dots and (C) dialysate N,P-Carbon dots

Figure 23. Absorption spectra of (A) dialysed or purified N,P-Carbon dots, (B crude N,P-Carbon dots and (C) dialysate N,P-Carbon dots

Figure 24. Emission spectra of (A) dialysed or purified N,P-Carbon dots, (B) crude N,P-Carbon dots and (C) dialysate N,P-Carbon dots

Figure 25 . FTIR spectra of dialysed or purified N,P-Carbon dots

Figure 26. (A) Absorption spectra of N,P-carbon dot and coacervate droplet and (B) Emission spectra of N,P-carbon dot and coacervate droplet

Figure 28. (A) Absorption and (B) fluorescence spectra of HSA capped gold nanoclusters. (C) Confocal and (D) FESEM image of HSA condensates @AuNCs

LIST OF SCHEMES

Scheme 1. Synthesis of ATP/PDADMAC coacervate nanodroplet.

Scheme 2. Synthesis of loaded coumarin 480 loaded ATP/PDADMAC droplet.

Scheme 3. Illustration of coacervate droplet Formation via QD-PDADMAC Nanocomposite Formation.

Scheme 4. Illustration of carbon dot formation by using ethylenediamine and citric acid and formation coacervate droplets in presence of polymer PDADMAC

Scheme 5. Illustration of N,P-Carbon dot formation by using o-Phenylenediamine and phosphoric acid and formation of coacervate droplets in presence of polymer PDADMAC.

Scheme 6. Illustration of synthesis of HSA capped Au NCs (20mg/ml HSA + 5 mM $HAuCl_4$).

LIST OF TABLES

Table 1. Data of average lifetime, lifetimes, pre-exponential factor and chi-square of each decay.

Table 2. Data of average lifetime, lifetimes, pre-exponential factor and chi-square of each decay of coumarin 480 in ATP/PDADMAC droplet.

NOMENCLATURE

a.u.	arbitrary unit
°C	degree Celsius
h	hour
μM	micromolar
mM	millimolar
nm	nanometer
M	molar
mL	millimolar
nm	nanometer
ns	nanosecond
mg	milligrams
rpm	revolution per minute

ACRONYMS

ATP	Adenosine 5′-triphosphate
C480	Coumarin 480
CD	Carbon dot
CTAB	Cetyltrimethylammonium bromide
CMC	Critical micelle concentration
DLS	Dynamic light scattering
FE-SEM	Field emission-scanning electron microscope
ND	Nano droplet
PL	Photoluminescence
PDADMAC	Poly(diallyldimethylammonium)chloride
SDS	Sodium dodecyl sulfate
TX-100	Triton X-100
UV	Ultraviolet
Vis	Visible

CHAPTER 1

1. INTRODUCTION

1.1 Solvation dynamics:

Solvation means stabilization of a probe molecules because of interaction of probe molecules with the solvent molecules present in the surrounding of probe molecules. Evidence said that solvation dynamics studied when the solvent is polar, and probe solute is dipolar or Ionic *[1]*. The solvation dynamics talks about how the solvent dipoles show rearrangement around charge or dipole created, is known as solvation dynamics. when polarity increases red shift of the absorption and emission maximum shown by such a molecule. A dipole is created when such a solute molecule in a solution is excited by a light pulse. Initially, solute dipole is remained oriented by solvent dipoles. Since the dipolar solute is in the excited state, it continuously emits energy of the excited dipole decreases when solvent dipoles reorient around solute dipole with increase in time *[2]*. Thus, emission maxima shift toward longer wavelength i.e., toward lower energy . This phenomenon is known as time dependent fluorescence stokes shift (TDFSS). Commonly used some solute probes are dyes coumarin 480 (C-480), coumarin 343 (C-343) and coumarin 314 (C-314), eosin Y, DCM (4-dicyanomethylene)-2-methyl- [6-p-(dimethyl amino) styryl]-4H-pyran), and 4-aminophtalimide(4-AP). The solvation dynamics is understable by the decay of the solvent correlation function C(t) calculated by given mathematical equation,

$$C(t) = \frac{v(t) - v(\infty)}{v(0) - v(\infty)}$$

Where, $v(0), v(\infty) and\ v(t)$ are peak frequency at time $0, \infty, and\ t$ respectively.

Researchers get interested to understand micro heterogeneous organized assemblies because of recent success in homogeneous solutions. some biological process happening in organized and restricted environment. An interest has been developed to understand how the organized assemblies affecting ultrafast process.

In this report, I wish to present the work on solvation dynamics of coumarin 480 in micelles which is already reported and explore the reported work mainly on the solvation dynamics of solute probe C480 dye inside the SDS micelle aggregates. An idea has been generated from this reported work and from some recent work in the solvation dynamics field; mainly inside the organized assemblies to further extend my study on solvation dynamics of solute probe C480 inside the Polymer/nucleotide droplet.

1.2 MICELLE

Surfactants form nearly spherical micelle aggregates when their concentrations exceed from a critical micellar concentration (CMC). The shape and size of a micelle are functions of the molecular geometry of its surfactant molecules and solution conditions such as surfactant concentration, temperature, pH, and ionic strength. The process of forming micelles is known as micellization. A micelle in water forms an aggregate with the hydrophilic “head” in contact with solvent around it, sequestering single-hydrophobic tail region in the centre of micelle *[4,33]*.

Micelles are widely used in industrial and biological fields for their ability to dissolve and move nonpolar substances through an aqueous medium, or to carry drugs.

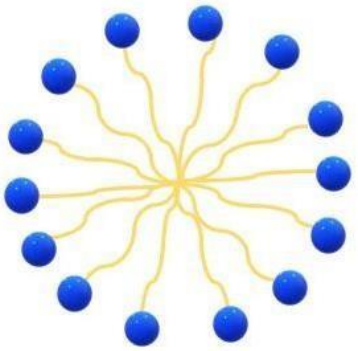

Figure 1. Structure of Micelle

In figure 1, blue spheres represent polar head group or hydrophilic head, and yellow lines represent hydrophobic tail.

1.3 STERN LAYER

The micelle core is "dry" and containing the hydrocarbon chain. At the periphery of micelles, there is shell (6-9Å) i.e., stern layer which contains polar group, the counterion and enough water quantity. This stern layer is quite polar *[4]*.

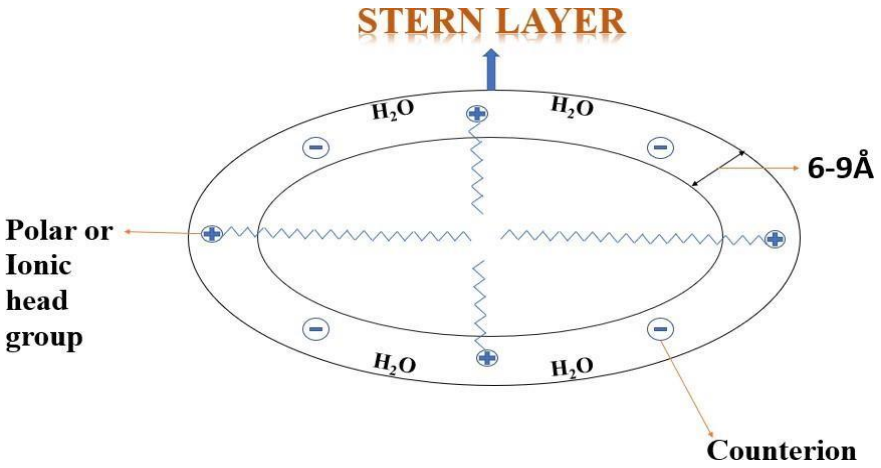

Figure 2. Structure of Stern layer

In recent experiments, we observed coumarin 480 was not giving time dependent stokes shift and does not fluorescence decay (wavelength dependent) in aliphatic hydrocarbon solvents. It is expected that coumarin 480 exhibit time dependent solvent shift in aliphatic hydrocarbon. But the question is what happens when solute probe coumarin 480 is reside in the stern layer.

1.4 Nucleotides

Nucleotides are organic molecules consisting of a nucleoside and a phosphate group. Nucleotides are composed of three subunit molecules which are covalently bonded: a nucleobase, a five-carbon sugar (ribose or deoxyribose), and a phosphate group. Nucleotides play a vital role in metabolism at a fundamental cellular level. In the form of adenosine triphosphate (ATP), nucleoside triphosphate, uridine triphosphate (UTP), cytedine triphosphate (CTP) and guansine triphosphate (GTP), they provide chemical energy throughout the cell that demand energy to perform many cellular functions. Nucleotides are negatively charged, and they are commonly used in the research of complex coacervation such as coacervate nanodroplets. Nucleotide (negatively charged) interact with the polyelectrolyte or polymer (positively charged) in the formation of coacervate nanodroplet.

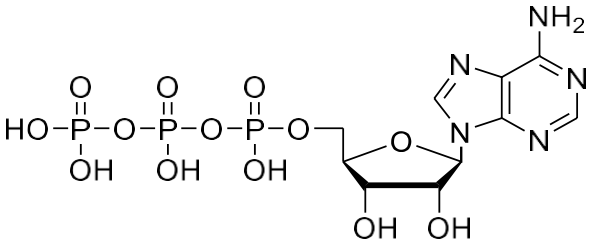

Figure 3. Structure of Adenosine triphosphate (ATP)

1.5 Nanoparticles

A nanoparticle usually defined as a very small entity or particle of size in nanometres specifically that have a size range of 1 nm to 100 nm. These nanoparticle are not easily detectable by the eye. These nanoparticle have different properties mainly chemical and physical properties to large matter counterparts.

Various types of nanoparticles consist of hundreds to thousands of entity like atoms.

1.5.1 Types of Nanoparticles

Developing nanoparticles with different structure**,** properties, and functions became a matter of an interest. In recent times, scientists show interest to develop organic nanoparticles due to their various applications like, OLED, medical diagnosis, and sensors.

Composition based classification of nanoparticles are given below:

1. Organic nanoparticles: Liposomes, Layered Biopolymer etc.
2. Inorganic nanoparticles: Quantum Dot, Carbon Dot, Gold Shell, Metal nanocluster etc.
3. Hybrid Nanoparticles: Polymer Hydrogel

To understand the solvation dynamics of confined system, firstly we synthesis the desired confined system. In our present work, we endeavour to understand the solvation dynamics of mainly three confined system namely, carbon nanodroplet, quantum nanodroplet and ATP nanodroplet. The nanoparticles used to synthesis these confined system is described below:

1. Carbon dots: This nanoparticle is the young member in the nanoworld. Carbon dots are generally spherical with average size less than 10 nm. These are derived from the organic material and stable in aqueous median, this is significant in biological view *[5].* Carbon dots have photophysical and photoluminescence properties which are used for bioimaging applications. Nanocomposite (multiphase solid)

material of carbon dots have enormous importance in biosensing simply, sensing, and medical research *[6].* Nano carbon dots are stable in broad range of ionic strength and pH. N-CDs has fluorescence property, emission maxima observed at 415 nm upon excitation of 340 nm. It is found that in aqueous media, carbon dots detect metals like, Hg^{+2} and Cu^{+2} *[7]*.

2. **Quantum dots:** In 1980, Russian physicist Alexey I. Ekimov first found these quantum dots in crystals of glass. After one more decade, colloidal quantum dots were discovered with some optical properties. Quantum Dots are little particles with size of few nanometers. Optical and electronic properties contrast from their larger particles. These are nanoscale particles, which are made up of semiconductor matters, they are bind either electron holes or electrons *[8].*

1.6 Nanoclusters

Nanoclusters are pile of atoms specifically it is a stack of atoms up to number of 150 atoms. Nanoclusters have core-shell shape contains a ligand shell and atomic core and they are smaller in shape and size up to 1-2 nm. They are photostable, good conductor of electricity and highly fluorescent. Atom present in the nanocluster show magnetic behaviour and more than that of larger quantity matter. Structural change in the structure of nanocluster leads to the formation of nanomagnet. Nanocluster can act as catalyst for example gold nanocluster because of their unique reactivity and they may also show optical properties. Nanoclusters have numerous applications because of unique magnetic, optical etc. properties. The valence band and conduction band are not continuous for longer time since they contain few 100 atoms, so the levels are not continuous, they are discrete *[9].*

1.6.1 Gold Nanocluster (AuNCs)

Gold nanoclusters are very small clusters that contains up to a few 1-150 atoms Au atoms of small size that has diameter lower than 2 nm. AuNCs have various types of optical properties like photodynamic,

photothermal conversion and photon absorption. Gold nanoclusters play an important role in various fields like, drug delivery, nanothermometry , imaging, vaccine development etc. They show different types of fluorescent behaviour in different type of capping ligands and luminescent property. AuNCs used as an important tool in various therapy like, photodynamic therapy, photothermal therapy, radiation therapy. The fluorescence intensity and position of emission maxima are depending on the chemical structure of gold nanocluster and synthetic procedure of AuNCs is very facile and they are quite stable *[9]*.

1.7 Polyelectrolytes or polymer

Polyelectrolytes are simply polymers which are water soluble due to the presence of ionic charge along their polymer chain. They are commonly used in the research of complex coacervation. They are classified as the linear or branched macromolecule chains which have many ionic groups in their structure. They are usually soluble in polar solvent, generally water. In positively (or negatively) charged polyelectrolyte solution, a single species polymer with random polydispersity and one species of counter-ions which are small ions with oppositively charged sign to that of macromolecular charge are present. The charge of counter-ion and macromolecular structure must be equivalent to attain the condition of electroneutrality. The commonly used polyelectrolytes are polyethyleneimine (PEI), poly(diallyl dimethylammonium chloride) (PDADMAC), and poly (sodium 4-styrene sulfonate) (SPS).

Few characteristics of PDAMAC polymer:

1. It is a high charge density cationic polymer.
2. Under the normal temperature, it is quite stable, unhydrolyzed, non-flammable with small excitability to skin and low toxicity.

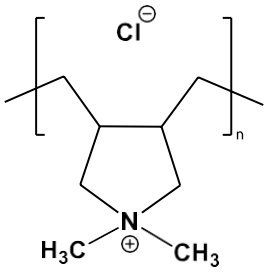

Figure 4. Structure of PDADMAC

1.8 Coacervate droplets

Coacervation is an electrostatically induced spontaneous liquid-liquid phase separation process between positively and negatively charged polyelectrolytes. Two phases of liquid coexist at the site of coacervation: a thick, polymer- rich phase (droplet phase or coacervative phase) and a highly diluted, polymer deficient phase defined as the dilute phase. As a result of this procedure, Spherical colloidal coacervate droplets with size ranging from a few nanometers to few micrometres are formed *[10]*.

Few characteristics of coacervates nanodroplets:

1. These are organic droplets formed by different organic molecules.

2. These are membrane-less nanodroplets.

3. These can uptake substances from surrounding.

Coacervates have attract researchers mind in artificial protocell investigations due to the preferential sequestration of biomacromolecules like dye, enzymes, and proteins and their intrinsic membrane-less crowding environment. Earlier, Mann and co-workers tested the preferential sequestration of the water insoluble solvatochromic dye, Nile red dye, into the PDDA/ATP inorganic droplet and found that the interior of these nanodroplets was much more polar as compared to DMSO but less hydrophilic than water. In this regard, in our present work, we investigated the behaviour of

coumarin 480 dye inside the ATP/PDADMAC droplet and understand the interior of droplet. Hence, we shall understand the solvation dynamics of coumarin 480 in ATP/PDADMAC droplet.

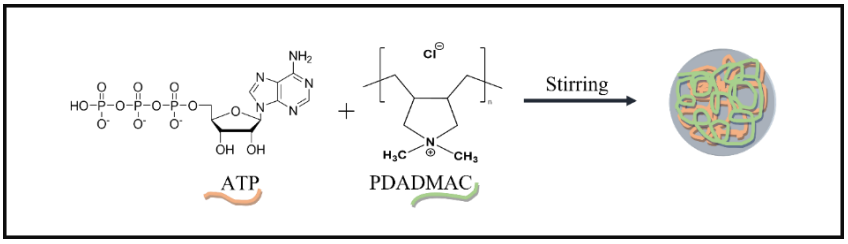

Scheme 1. Synthesis of ATP/PDADMAC coacervate nanodroplet.

1.8.1 Quantum dot droplets

These droplets are spherical coacervate droplets with size ranging from a few nanometers to few micrometres *[11]*. Earlier Mann and co-workers show the demonstration of coacervation of PDADMAC polymer and polypeptides with many mononucleotides which are anionic in nature *[12-13].* Tirell and workers talk about the mechanism of formation of nanodroplet with various polypeptides (oppositive charged) and polymer in aqueous phase *[14]*, In recent times of study, Hwang et al. report the demonstration of coacervate of two cationic polyelectrolytes and conclude that driven force of coacervation is cation – pi interactions of short range *[15]*. Although past studies provide information of coacervate driven droplets synthesised from organic molecules but quantum nanodroplets are hybrid droplets because they are generated from the inorganic and organic matter. Q-NDs are hybrid nanodroplets and have membrane free interior structure. Due to this membrane free structure, Q-NDs are used in artificial protocol research area .

These Q-NDs are synthesised by the simple mixing of CdTe-QDs and polyelectrolyte PDADMAC in water due to electrostatic interaction between negatively charged CdTe-QDs and positively charged polyelectrolyte PDADMAC. Hydrophobic and electrostatic interaction between outside molecule and nanodroplets accomplished the sequestration activity, specific sequestration of large range of

substrates like, organic molecule, enzymes, and proteins *[16]*. Inside these nanodroplets, sequestered enzymes show catalytic action *[17]*. Due to this property, coacervate nanodroplet are auspicious bioreactors. These hybrid quantum nanodroplets are retaining the character or quality of inorganic and organic correspondent, it is expected that the application and stability of structure are increased at that same instance. These quantum nanodroplets are exhibiting two photon fluorescence, which may be used in various applications like, tissue imaging and vivo cell.

1.8.2 Carbon dot droplets

Carbon dot droplets are result of coacervation having spherical shape with size ranging from a few nanometers to few micrometres. In past, there is development of nanocarrier setup made up of liposomes but there loading capacity of drugs is much poor, short retention period and leakage of loaded drugs instantly after loading is another considerable limitation of these types of nanocarriers made up of liposomes. In this regard, coacervate nanodroplets like, carbon dot nanodroplet provide a distinctive and special advantage because of their membrane less structure *[18-19]*.

The stability of this carbon nanodroplet is impacted by change in pH, ionic strength, and equilibrium time. There are two different types of nanodroplets are formed upon changing the equilibrium time i.e., at 1hr of equilibration, small nanodroplets are formed while at 18 hr of equilibration, large nanodroplets are formed. These nanodroplets are not stable below pH 5 while they are quite stable in a range of pH 6 - *12*. Similarly, in media of high ionic strength, disassembly of nanodroplets is reported. Anti-cancer drugs and organic dyes are preferential sequestered inside these droplets due to their membrane less structure *[20]*.

CHAPTER 2

2. EXPERIMENTAL PROCEDURE

2.1 MICELLES

2.1.1 Materials: Hexadecyltrimethylammonium bromide (CTAB) (> 96.0%), Triton X-100 reduced (TX-100, AR grade), sodium dodecyl sulphate (SDS) (> 98.5%), coumarin 480 (MW =255.32 gm/mL) were bought from Sigma-Aldrich and DI water was taken from distillation unit.

2.1.2 Preparation of micelles: Purified Surfactants (2 mM TX-100, 3.5 mM CTAB, and 32 mM SDS) were added in DI water (pH 6.8) separately in 15 mL glass vials after that sonicate the samples of CTAB and SDS for 10 minutes for properly dissolving of surfactants, further put all three samples for 30 min incubation.

2.1.3 Assembly formation (or assimilation): Solute probe 2.08 μM coumarin 480 dye was added in the prepared micelle results to assembly formation.

2.2 ATP/PDADMAC droplet

2.2.1 Materials: All used chemicals are purchased from Sigma Andrich. Adenosine 5′-triphosphate (ATP) disodium salt hydrate(99%), poly(diallyl dimethylammonium chloride) (PDADMAC) (20 wt. % in water), sodium hydroxide (NaOH), coumarin 480 (MW: 255.32 gm/mL and DI water was obtained from a distillation unit purifier system.

2.2.2 Preparation of ATP/PDADMAC coacervate droplet: Nucleotide Adenosine 5′-triphosphate (ATP) and polyelectrolyte/polymer poly(diallyl dimethylammonium chloride) (PDADMAC) was added to DI water to form an aqueous solution. To ATP solution, NaOH was added to maintain the pH 8 for the better coacervation of nucleotide and polyelectrolyte and put the aqueous

solution of ATP and PDADMAC at incubation for 40 minute. See synthesis of droplet in scheme (I).

2.2.3 Preparation of coumarin 480 loaded ATP/PDADMAC droplet: 1.66 µL coumarin 480 dissolved in ethanol was added to droplet and give around 2 hr incubation for proper loading of dye inside the droplet.

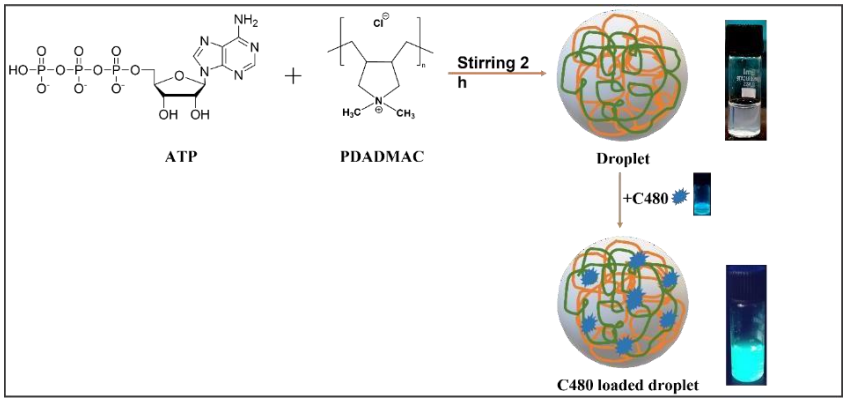

Scheme 2. Synthesis of loaded coumarin 480 loaded ATP droplet.

2.3.1 Quantum dot droplet

2.3.1 Materials: Cadmium chloride ($CdCl_2$) was purchased from sigma aldrich, poly(diallyldimethylammoniumchloride) (PDADMAC), Trisodium citrate dihydrate ($Na_3C_6H_5O_7.2H_2O$), Sodium tellurite (Na_2TeO_3), Mercaptosuccinic acid (MSA), Sodium borohydride ($NaBH_4$), the Pur-A-Lyzert dialysis kit was bought from Sigma-Aldrich company and DI water was obtained from a distillation unit purifier system.

2.3.2 Preparation of quantum dot: 0.04 M cadmium chloride in 4 mL DI water was diluted to a 50 mL flask and then), trisodium citrate dihydrate ($Na_3C_6H_5O_7.2H_2O$) (100 mg) Sodium tellurite (0.01 M, 1 mL), MSA (50 mg), and $NaBH_4$ (100 mg) were added with stirring continuously When there is appearance that the colour changed to green, the flask was connected to condenser and give reflux for 0.5 and 5.0 h to get green and quantum dots , respectively then the mixture

obtained was dialysis against DI water and at last purified sample was kept at cold place *[21]*.

2.3.3 Preparation of quantum dot droplet: Quantum dot droplets were prepared by using prepared quantum dot (80nM) and cationic polymer PDADMAC (33µM) in deionised (DI) water and put for equilibration for 4 hr at normal room temperature to get stabilised spherical droplet.

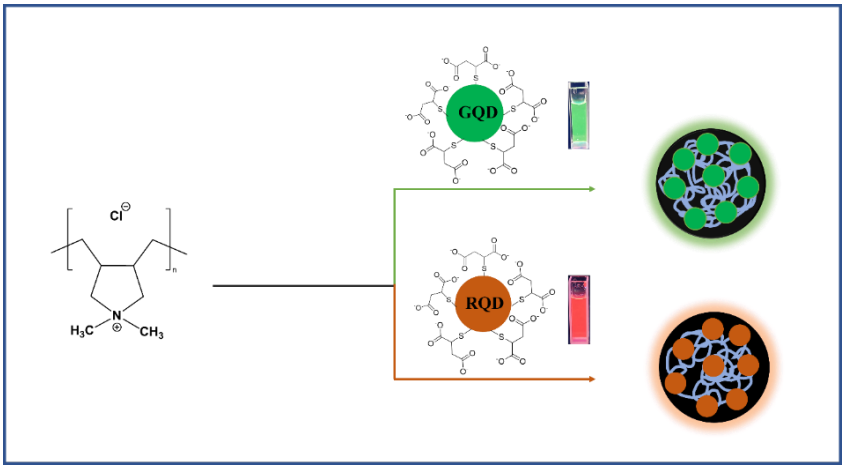

Scheme 3. Illustration of coacervate droplet Formation via QD-PDADMAC Nanocomposite Formation.

2.4 Carbon dot droplet

2.4.1 Materials: Citric Acid monohydrate (99.5%) bought from Merck (Germany) . PDADMAC, (poly- (diallyldimethylammonium chloride)) (20 wt. % in water), MW = 100k−200k, Ethylenediamine (EDA, 99.5%), sodium hydroxide(NaOH), deionised water (DI water) was obtained from a distillation unit purifier system.

2.4.2 Preparation of carbon dot: Carbon dots are synthesised by hydrothermal methodology *[22-23]*. In brief, first citric acid (1.015 g) was dissolved in 10 mL of DI water by sonicate it for 10-15 minutes. After proper complete dissolution of citric acid in DI water, ethylenediamine (335 µL) was properly added slowly to it and further sonicating the solution for 10-15 minutes. Then a dissolved solution

formed was transfer to a Teflon-padded autoclave (25 mL) and put the prepared solution in the oven for 5 hours and set the temperature to 200 °C. After 5-hour, reactor was cooled naturally at room temperature, and prepared solution was dialysed by using a Pur-A-Lyzer (MWCO 3.5 kDa) to remove free reactants from solution.

2.4.3 Preparation of carbon dot droplet: Carbon dot droplet were prepared by using prepared carbon dot (0.06 mg/mL) and cationic polymer PDADMAC (32μM) at pH 10 adjusted by the 0.1M NaOH put for equilibration for 16 hour at nor room temperature to get stabilised spherical droplet.

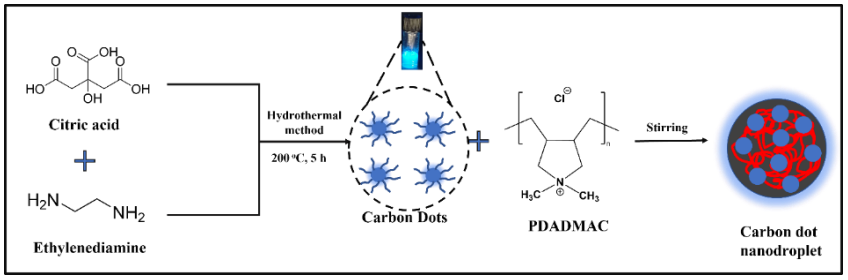

Scheme 4. Illustration of carbon dot formation by using ethylenediamine and citric acid and formation of coacervate droplets in presence of cationic polymer PDADMAC**.**

2.5 N,P-Carbon dot droplet

2.5.1 Materials: ortho-Phenylene diamine was purchased from Sigma Aldrich and phosphoric acid (H_3PO_4). Deionised (DI) water was obtained from a distillation unit purifier system and used in all experiments.

2.5.2 Synthesis of N,P-CDs: N,P-CDs were synthesised by taking 100 mg ortho-Phenylene diamine in 40 mL autoclave chamber that contains 13.5 mL of DI water after this add phosphoric acid (1.5 mL) dropwise into this autoclave chamber. Then after, this reaction mixture put in oven at 160 °C for 6 hr. After this thermolysis, autoclave

chamber cools down naturally at room temperature. Then, product was centrifuged at 15,000 rpm for 15 min then filter product by using syringe (0.22 μm-pore filter). Then in last step, N,P-CDs purified using dialysis kit *[24]*.

2.5.3 Synthesis of N,P-Carbon dot droplets: N,P-Carbon dot droplets were synthesised by using 100 μL of purified N,P-CDs and 350 μM PDADMAC in 3 mL of DI water maintaining pH 10 adjusted by using 0.1M NaOH and put for equilibration for 16 hour at room temperature to get stabilised spherical droplets.

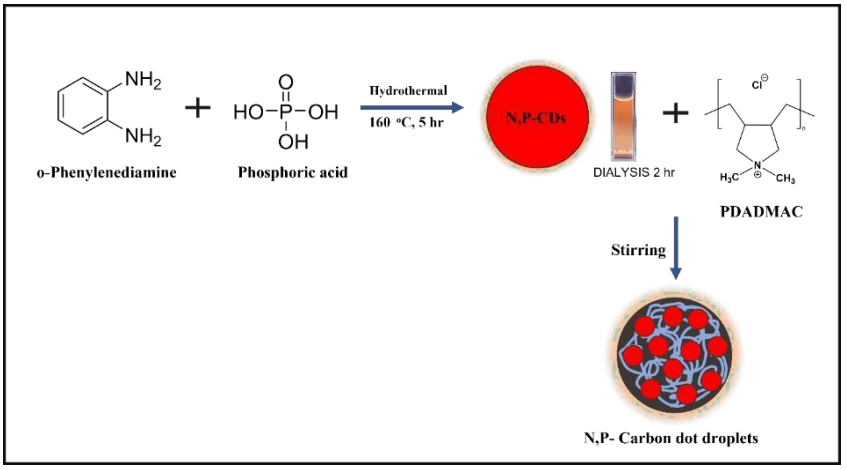

Scheme 5. Illustration of N,P-Carbon dot formation by using o-Phenylenediamine and phosphoric acid and formation of coacervate droplets in presence of cationic polymer PDADMAC.

2.6 Gold Nanocluster

2.6.1 Materials: Human serum albumin (HSA), cell culture tested was purchased from himedia, Chloroauric acid ($HAuCl_4$), Poly(ethylene glycol) Bio ultra 8,000 (PEG) was purchased from sigma Aldrich, Sodium hydroxide (NaOH), deionised water (DI water) was obtained from a distillation unit purifier system.

2.6.2 Preparation of HSA capped gold nanoclusters: HSA capped AuNCs were synthesised by using Human serum albumin HSA

(20mg/mL) and Chloroauric acid ($HAuCl_4$, 5 mM) in DI water maintaining pH 9.5 by adding 0.1 M sodium hydroxide and stir the solution for 24 h at 37 °C then solution was dialysed for 4 hr by using dialysis kit .

2.6.3 Preparation of HSA condensates @ gold NCs: HSA Condensates @ gold nanoclusters were synthesised by taking HSA capped gold NCs in the presence of 10% PEG 8000 at 37 °C and incubated for 1 day.

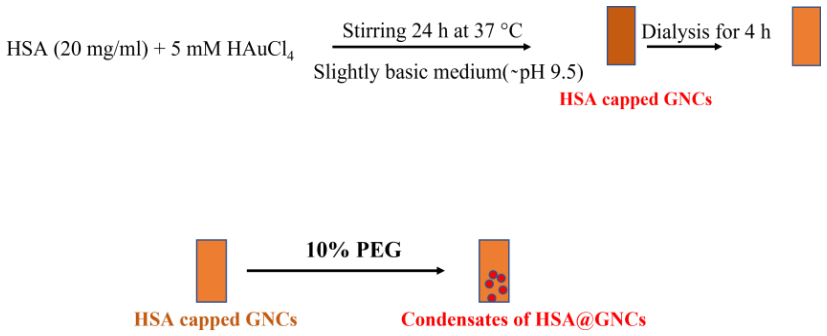

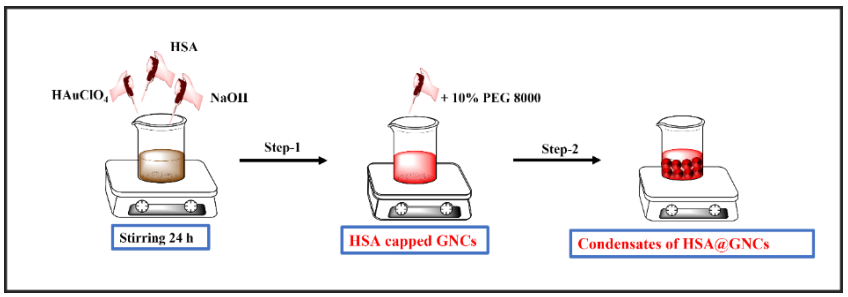

Scheme 6. Illustration of synthesis of HSA capped Au NCs (20 mg/ml HSA+ 5 mM $HAuCl_4$).

2.7. INSTRUMENTATION

2.7.1 UV-Visible Spectrophotometer

Absorption spectra was recorded in a cuvette using a Perkin Elmer lambda 750 spectrophotometer by taking base line of water to subtract the absorption of water.

2.7.2 Fluorescence spectrofluorometer

Emission spectra were recorded in a cuvette (10*10 mm) using by using a Fluoromax Spectrofluorometer (Horiba Jobin Yvon, modelFM-100) slit width at 2 nm.

2.7.3 Time-correlated single photon counting (TCSPC)

TCSPC set up from IBH Horiba Jobin Yvon (USA) was used to collect lifetime of decay range from wavelength 450 nm to 600 nm at intervals of 10 nm and slit width less than or equal to 4 nm. The excitation wavelength for time-resolved and steady state study is 405 nm. All the decays were analysed using the software named IBS DAS 6.0. Data was fitted to biexponential or triexponential using analysis software. Ludox solution was used to record the decay of instrument response function.

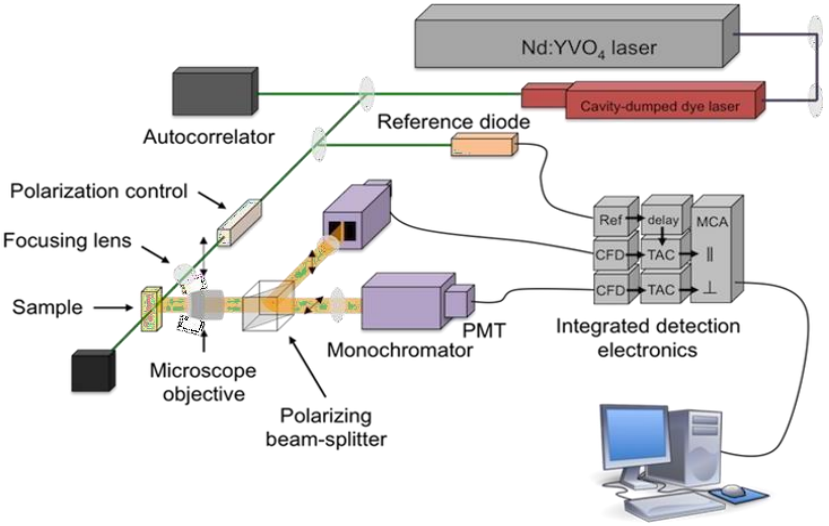

Figure 5. Diagram of TCSPC

2.7.4 Field Emission Scanning Electron Microscopy (FE-SEM)

The nanodroplet were confirmed by using the FE-SEM technique. The FE-SEM, supra 55 Zeiss was used to collect SEM images of nanodroplet. Prepared sample was drop casted on SEM slides overnight and gold coating on slides before performing FE-SEM technique.

2.7.5 Confocal Fluorescence Microscopy

Confocal images of nanodroplets were detected by confocal microscope (Olympus model no.FV1200MPE, IX-83) by using oil immersion objective (100X, 1.4 NA). To excite samples using desired dichroic a 405 nm laser source was used and in the optical path, filters are used. The samples are drop casted on confocal slides.

2.7.6 Thermogravimetric Analysis (TGA)

The water content inside the ATP/PDADMAC droplet at pH 8 was detected using thermogravimetric analysis (TGA). The water content inside droplet was known by knowing the weight loss at 110 °C , with subsequent uphold the temperature at 110 °C for around 5 hour and after 5 hour increase the temperature up to 800 °C. The concentration of ATP and PDADMAC is 30 mM and molar ratio of ATP/PDADMAC is 1:1 and separate out the droplets by centrifuging the sample at 5000 rpm for 15 minutes to get the coacervate thick phase.

2.7.7 Fourier-transform infrared spectroscopy (FTIR)

This technique is used for the identification of different types of functional groups present on the nanoparticles. Infrared spectra were noted by Bruker spectrometer (Tensor-27) by using thin pellet mainly thin KBr pellet. All Infrared spectra(IR) were recorded in range of wavenumber 4000 cm^{-1} to 800 cm^{-1} on an average of 10 scans.

CHAPTER 3

3. Results and Discussion

3.1 Micelles

3.1.1 Steady state spectrum: C-480 exhibits an emission maxima at around 490 nm in water. When concentration of surfactant is less than cmc, emission spectra of coumarin 480 remain unchanged or negligible change but if concentration of surfactants is more than cmc, the emission spectra of coumarin 480 changed exhibit shift to 475 nm in CTAB and SDS and 470 nm in TX-100 which indicates solute probe coumarin 480 is transferred from aqueous medium to polar micelle which is less polar. Emission peak of coumarin 480 in micelles is like that of alcohol medium which is homogeneous. Some parts of solute probe experience lower polarity as compared to bulk water.

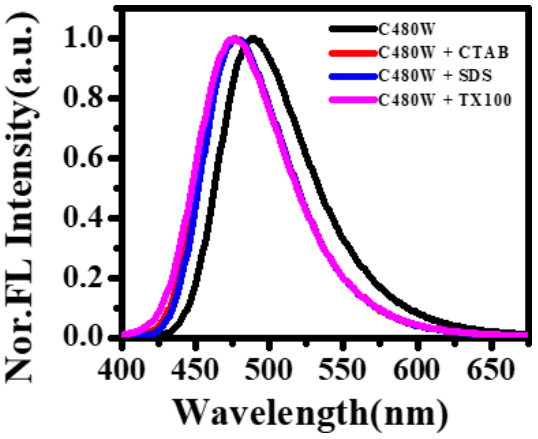

Figure 6. Emission spectra of probe coumarin 480 in water, 3.5 mM CTAB, 2 mMTX-100, and 32 mM SDS.

SDS MICELLE

3.1.2 Steady state spectrum

In aqueous media, emission maxima of coumarin 480 show blue shift from 490 nm to 475 nm in presence of SDS micelle at excitation of 390 nm, it indicates that coumarin 480 is transfer from polar region to

low polar micelle area. In ,micelle region, probe solute i.e., coumarin 480 experiences lower polarity in comparison to bulk water.

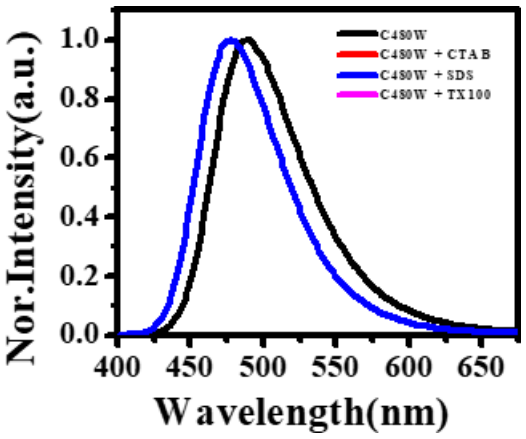

Figure 7. Emission spectra of probe coumarin 480 in water and 32mM SDS micelle.

3.1.3 Time-resolved studies

To obtain information about solvation dynamics of coumarin 480, the time resolved emission spectra (TRES) of probe coumarin 480 in Water in presence of sodium dodecyl sulphate (SDS) above the critical micelle concentration see figure(8). Few dyes do not exhibit time-resolved emission spectra in hydrocarbon core while solvation of these dyes is fast in bulk water observed in our work. Reconstruct the response function for extracting the time constant of coumarin 480 in the stern layer of SDS micelle.

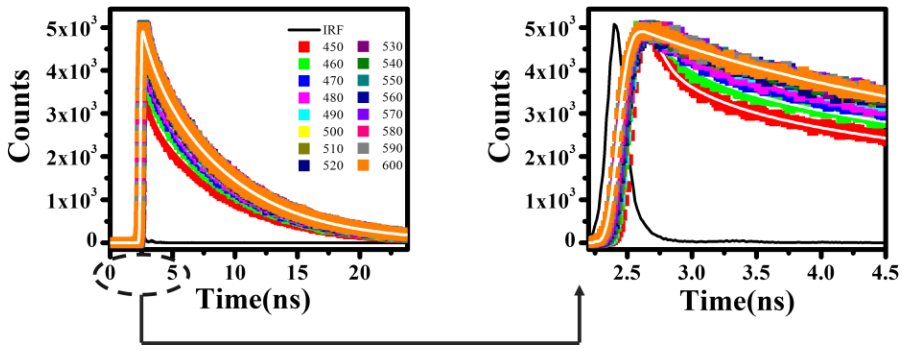

Figure 8. Lifetime Decays of solute probe coumarin 480 in 32 mM SDS at range of wavelength 450-600 nm.

Wavelength(nm)	τ_1 (ns)	a_1	τ_2(ns)	a_2	τ_3(ns)	a_3	$\tau_{avg.}$(ns)	χ^2
450	0.46	0.15	5.99	0.35	0.072	0.50	2.22	1.08
460	0.40	0.10	6.02	0.24	0.029	0.66	1.49	1.07
470	0.48	0.11	6.04	0.39	0.039	0.50	2.42	1.06
480	0.52	0.10	6.04	0.45	0.042	0.44	2.80	1.01
490	0.55	0.03	6.05	0.13	0.014	0.85	0.79	1.08
500	0.53	0.08	6.03	0.41	0.036	0.51	2.53	1.06
510	0.69	0.10	6.07	0.66	0.073	0.25	4.07	1.09
520	1.09	0.03	6.06	0.80	0.32	0.17	4.96	1.11
530	0.55	0.03	6.05	0.13	0.011	0.85	0.79	1.08
540	0.59	0.08	6.06	0.58	0.040	0.34	3.56	1.01
550	0.52	0.03	6.07	0.17	0.011	0.81	1.03	1.06
560	1.17	0.04	6.10	0.82	0.3	0.14	5.12	1.06
580	1.18	0.00	4.92	-0.50	4.93	0.50	4.92	1.11
600	1.79	-0.42	5.01	0.53	1.11	0.01	4.86	1.10

Table 1. Data of average lifetime, lifetimes, pre-exponential factor and chi-square of each decay.

3.1.4 Construction of TRES:

Time-resolved emission spectra of SDS micelle is obtained by using given mathematical equation *[25]*:

$$I(v,t_k) = I_{ss}(v)\frac{\sum_{i=1}^{n} a_i\,(v)e^{\frac{-t_k}{c_i(v)}}}{\sum_{i=1}^{n} a_i(v)r_i(v)}$$

Where $I_{ss}(v)$ represent fluorescence intensity of steady state.

$I(v,t_k)$ represent fluorescence decay.

$\sum_{i=1}^{n} a_i(v)r_i(v)$ represent average lifetime of each decay.

3.1.5 Interpretation of time resolved emission spectra (TRES):

TRES in figure (9) shows that intensity get decreases with the time and minor differences in the shape of spectrum at different range of time are invisible because intensity is decreasing continuously.

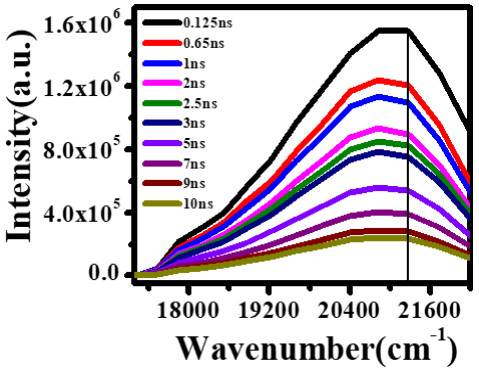

Figure 9. Time resolved emission spectra of coumarin 4800 in SDS micelle at different times.

To construct the time response function, we construct TRES with normalised fluorescence intensity and wavenumber at different times see figure (10)

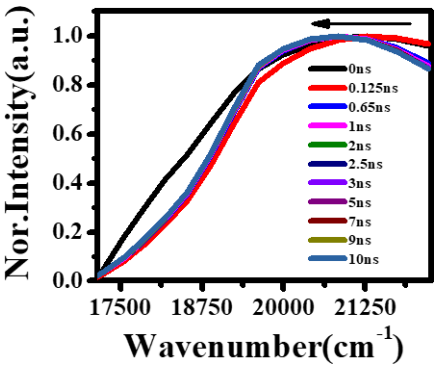

Figure 10. TRES of coumarin 480 in SDS micelle.

Interpretation of TRES: As we clear see from the time resolved emission spectra (TRES) figure (10) with increasing the time, blue shift is observed represented by arrow or stoke sift is observed with time.

3.1.6 Construction of time-response function C(t)

To obtain the time constant of coumarin 480's solvation dynamics in the stern layer of micellar region, we construct the response function C(t) by using the given mathematical equation.

$$C(t) = \frac{v(t) - v(\infty)}{v(0) - v(\infty)}$$

Where, $v(0), v(\infty) and\ v(t)$ are peak frequency at time $0, \infty, and\ t$ respectively, Figure(11) shows decay of C(t)for SDS micelle.

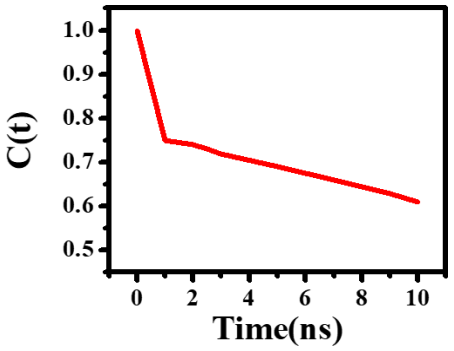

Figure 11. C(t) of coumarin 480 in 32 mM SDS.

We can say that solvation dynamics in micelle is faster than solvation dynamics observed in water pool of reverse micelle (2-8 ns). The observed solvation dynamics of water in in stern layer (180-350 fs) is slower than in ordinary water (310 fs). The solvation behaviour of the ionic micelle is different than neutral or cation micelles because of presence of counterion in ionic SDS micelle.

3.2 ATP/PDADAMAC droplet

3.2.1 Characterisation of ATP/PDADMAC droplet

The synthesized ATP droplet have been characterized by field electron scanning electron microscopy (FE-SEM) and Confocal laser scanning microscopy (CLSM) see figure(12).

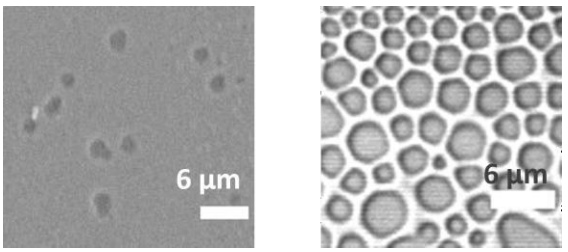

Figure 12. FE-SEM and confocal image of ATP/PDADMAC droplet.

3.2.2 Characterisation of coumarin 480 loaded ATP/PDADMAC droplet

The synthesised ATP/PDADMAC droplet have been characterised by microscopic confocal images see figure (13).

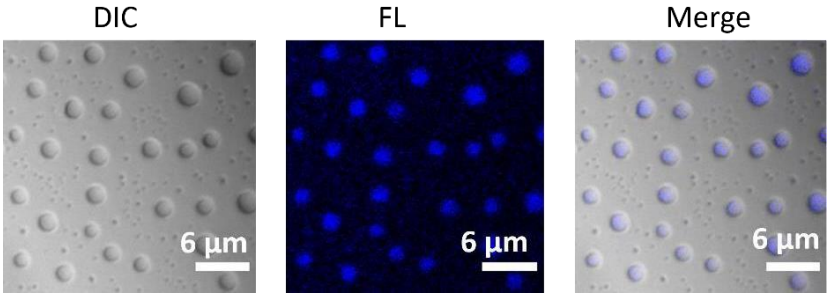

Figure 13. Confocal images of coumarin 480 loaded ATP droplet.

3.2.3 UV-Visible spectra: Absorption spectra of coumarin 480 loaded ATP/PDADMAC droplet shows no shift in absorption maximum with respect to time from 0 to 160 minute. We have not concluded much from absorption spectra see figure (14).

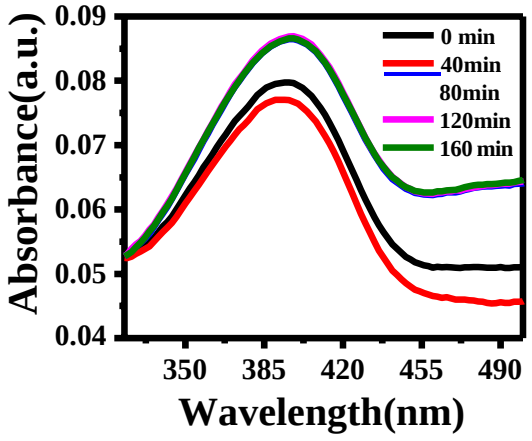

Figure 14. Absorption spectra of coumarin 480 loaded ATP/PDADMAC droplet.

3.2.4 Steady state emission spectra

Emission spectra of coumarin 480 in water and ATP/PDADMAC droplet shows emission maximum at 490 nm at excitation of 390 nm but no stoke shift shown in water and ATP droplet.

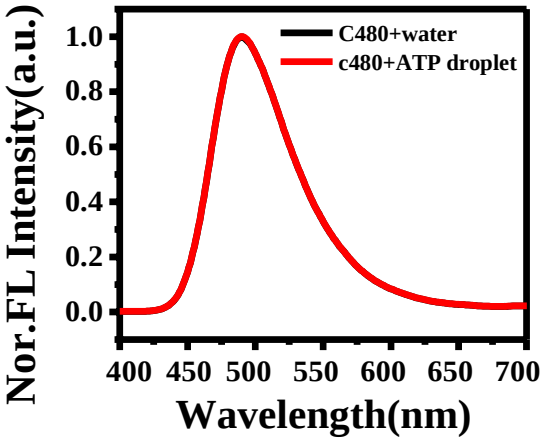

Figure 15. Emission spectra of coumarin 480 in water and ATP droplet

3.2.5 Time dependent emission spectra

Emission spectra of coumarin 480 in ATP/PDADMAC droplet shows a time dependent shift in emission maximum at excitation of 390 nm. This time dependent shift in emission maximum of coumarin 480 may be because of time dependent loading of coumarin 480 inside droplet. From figure (16), We can say that coumarin 480 dye is loaded inside ATP droplet with respect to time, it means coumarin 480 loaded inside the ATP/PDADMAC droplet.

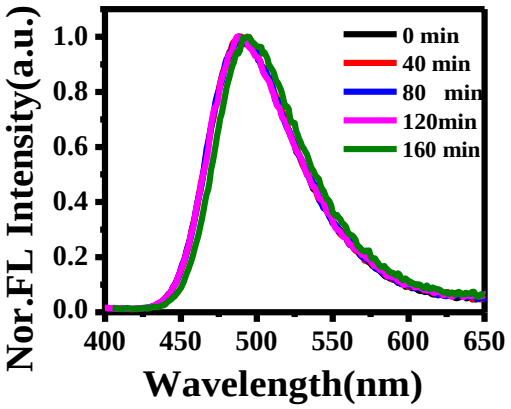

Figure 16. Emission spectra of coumarin 480 in ATP/PDADMAC droplet at different interval.

3.2.6 Time-resolved studies

To obtain information about solvation dynamics of coumarin 480, the time resolved emission spectra (TRES) of probe coumarin 480 in ATP/PDADMAC are constructed at different times from decays taken in a range of wavelength from 440 to 600 nm at interval of 10 nm. Reconstruct the response function for extracting the time constant of coumarin 480 (figure 17).

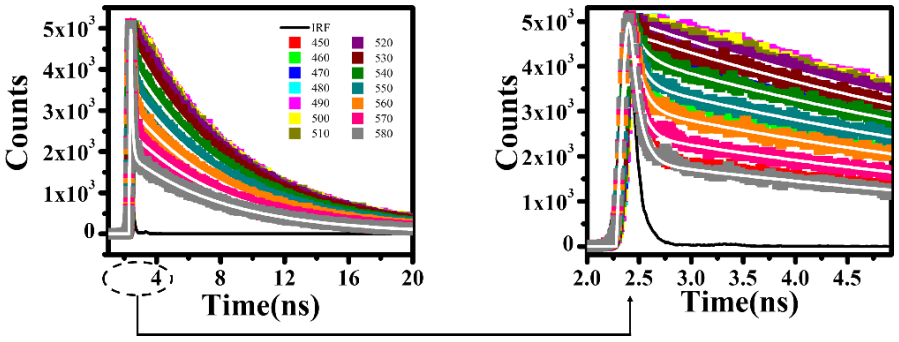

Figure 17. Decays of solute probe coumarin 480 in ATP/PDADMC droplet at range of wavelength 440-600 nm.

Wavelength(nm)	τ_1 (ns)	a_1	τ_2 (ns)	a_2	$\tau_{avg.}$(ns)	χ^2
450	0.08	0.78	5.82	0.22	1.34	1.14
460	0.08	0.51	5.84	0.49	2.90	1.17
470	0.065	0.34	5.85	0.66	3.91	1.09
480	0.45	-0.04	5.83	0.96	5.64	1.09
490	2.82	-0.03	5.77	0.97	5.67	1.16
500	2.65	-0.04	5.78	0.96	5.69	1.15
510	2.75	-0.01	5.85	0.99	5.83	1.07
520	2.72	-0.01	5.84	0.99	5.84	1.13
530	2.77	0.01	5.88	0.99	5.88	1.07
540	0.11	0.25	5.86	0.75	4.41	1.05
550	0.09	0.46	5.87	0.54	3.18	1.05
560	0.08	0.61	5.84	0.39	2.34	1.04
570	0.08	0.72	5.83	0.28	1.67	1.10
580	0.081	0.80	5.81	0.20	1.24	1.14

Table 2. Data of average lifetime, lifetimes, pre-exponential factor and chi-square of each decay of coumarin 480 in ATP/PDADMAC droplet.

3.2.7 Construction of TRES

Time-resolved emission spectra of SDS micelle is obtained by using given mathematical equation *[25]*.

$$I(v, t_k) = I_{ss}(v) \frac{\sum_{i=1}^{n} a_i\,(v) e^{\frac{-t_k}{c_i(v)}}}{\sum_{i=1}^{n} a_i(v) r_i(v)}$$

Where $I_{ss}(v)$ represent fluorescence intensity of steady state.

$I(v, t_k)$ represent fluorescence decay.

$\sum_{i=1}^{n} a_i(v) r_i(v)$ represent average lifetime of each decay.

3.2.8 Interpretation of time resolved emission spectra (TRES)

TRES in figure (18) shows that intensity get decreases with the time and differences in the shape of spectrum at a various range of time are invisible because intensity is decreasing continuously.

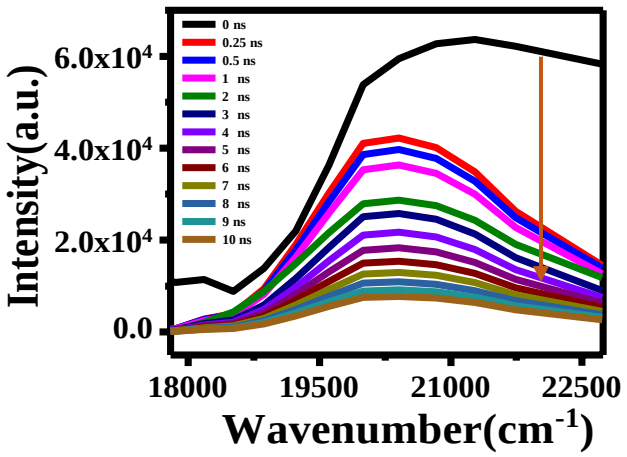

Figure 18. Time resolved emission spectra of coumarin 480 in ATP/PDADMAC droplet.

To construct the time response function, we construct TRES with normalised fluorescence intensity and wavenumber at different times see figure (19).

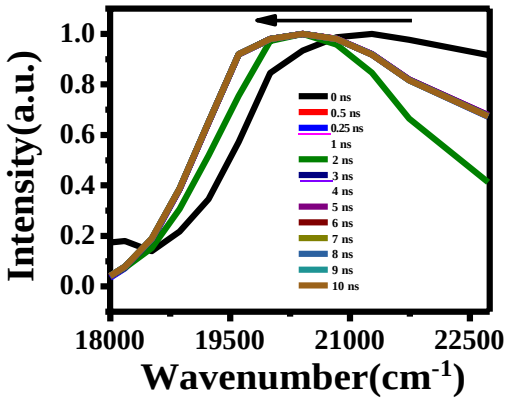

Figure 19. TRES of coumarin 480 in ATP/PDADMAC droplet.

3.3 Quantum dot droplet

3.3.1 Characterization of green quantum dot droplets

The synthesised green quantum droplets were characterised by using UV-vis spectroscopy, fluorescence spectroscopy, and Confocal laser scanning microscopy (CLSM). The synthesised green quantum dots and green quantum droplets show absorption maxima at 490 nm in UV-vis spectroscopy (Figure 20A). The emission maxima of green

quantum dot show shift from 525 nm to 532 nm after addition of polymer PDADMAC with red shift of wavelength 8 nm upon excitation at 450 nm and fluorescence intensity of quantum dot is decreasing significantly due to quenching in presence of polymer PDADMAC (Figure 20B). Figure 20C shows the confocal images of green quantum droplets in CLSM.

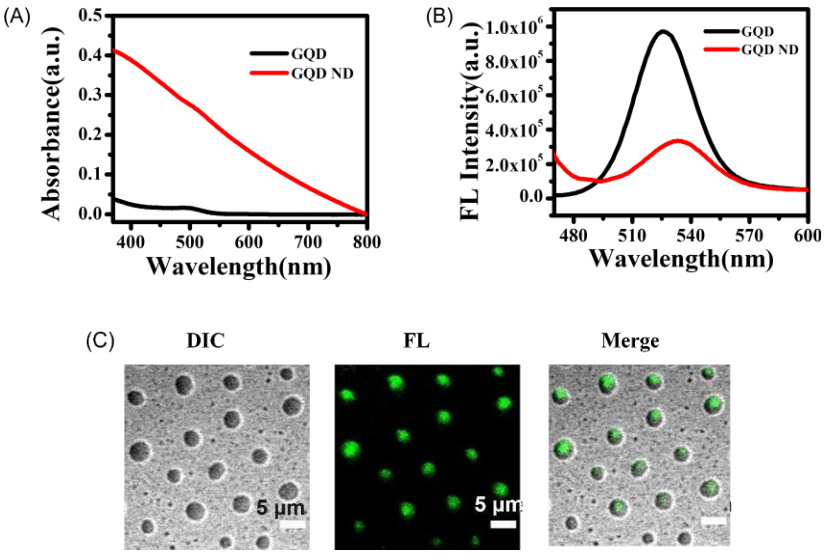

Figure 20. (A) Absorption spectra, (B) Fluorescence spectra of green quantum dots and green quantum droplets, and (C) Confocal images (DIC, FL, and merge) of green quantum droplets.

3.3.2 Characterization of red quantum dot droplets

The synthesised red quantum droplets were characterised by using UV-vis spectroscopy, fluorescence spectroscopy, and Confocal laser scanning microscopy (CLSM). The synthesised red quantum dots and red quantum droplets show absorption maxima at 585 nm in UV-vis spectroscopy (Figure 21A). The emission maxima of red quantum dot show shift from 620 nm to 628 nm after addition of polymer PDADMAC with red shift of wavelength 8 nm upon excitation at 450 nm and fluorescence intensity of quantum dot is decreasing significantly due to quenching in presence of polymer PDADMAC

(Figure 21B). Figure 21C shows the confocal images of red quantum droplets in CLSM.

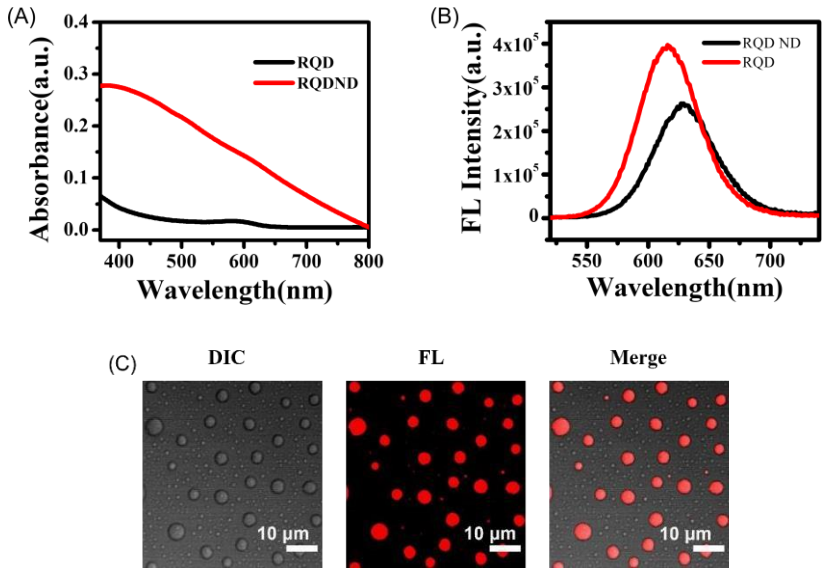

Figure 21.(A)Absorption spectra, (B) Fluorescence spectra of red quantum dots and green quantum droplets, and (C) Confocal images (DIC, FL, and merge) of red quantum droplets.

3.4 Carbon dot droplets

3.4.1 Characterization of green quantum droplets

The synthesised droplets were characterised by using UV-vis spectroscopy, fluorescence spectroscopy, and confocal microscopy (CLSM). The synthesised carbon dots and carbon dot droplets show absorption maxima at 339 nm in UV-vis spectroscopy (Figure 22A) and emission maxima at 448 nm upon excitation on 365 nm in fluorescence spectroscopy (Figure 22B). Figure 22C displays the confocal images (DIC, FL, Merge), DIC image show the presence of stabilised coacervate droplet while in FL, blue colour emission indicate that carbon dots are distributed uniformly inside these coacervated carbon dot droplets.

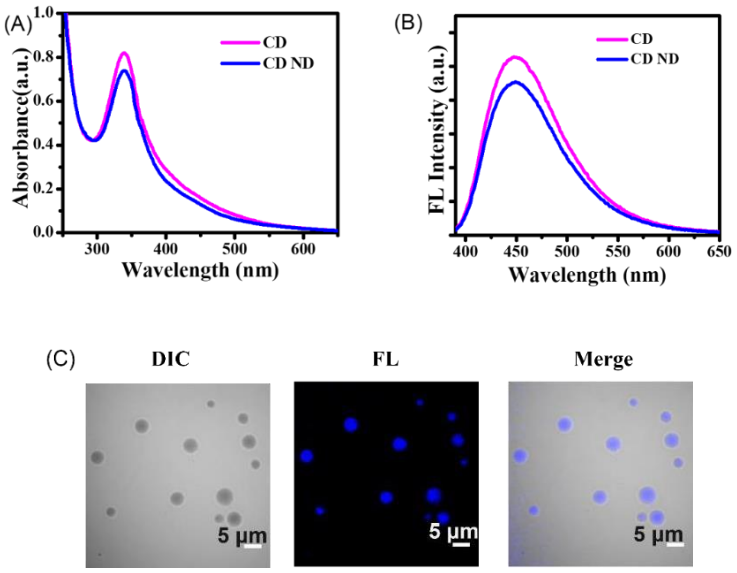

Figure 22. (A) Absorption spectra, (B) Fluorescence spectra of carbon dots and carbon dot droplets, and (C) Confocal images (DIC, FL, and merge) of carbon dot droplets.

3.5 N,P-Carbon dot droplet

3.5.1 Characterization of N, P-Carbon dots: The synthesised coacervate droplets were characterised by using UV-vis spectroscopy, fluorescence spectroscopy, and Fourier transform infrared spectroscopy (FTIR). Absorption spectra of dialysed or purified N,P-Carbon dots, crude N,P-Carbon dots and dialysate N,P-Carbon dots were recorded by using UV-vis spectroscopy as shown in figure 23A, B and C respectively. Emission spectra of dialysed or purified N,P-Carbon dots, crude N,P-Carbon dots and dialysate N,P-Carbon dots were recorded at different wavelengths (280-600 nm) by using fluorescence spectroscopy as shown in figure 24 A, B and C respectively. IR spectra of N,P-Carbon dots were recorded by using Fourier transform infrared spectroscopy as shown in figure 25. The absorption spectra of synthesized N,P-CDs displays absorption band at 404 nm, which belong to n-π* transition of C=N, C=O etc. and peak around 470 nm can belongs to nitrogen containing molecular state as reported earlier [26-27]. N,P-Carbon dots display a wide absorption shoulder in region of longer wavelengths with maxima at around 576

and 610 nm, respectively. However, this wide band is not found for pure N-Carbon dot. So, this absorption band in the region of longer wavelength may be related to functional groups of phosphorous containing surface and their noncovalent interactions with the solvent media in surrounding *[28-29]*. N,P-CDs show PL emission behaviour at different excitation wavelengths. The emission maxima have been found at 621, 576, and 387 nm at excitations of 560, 400 and 340 nm wavelength, respectively. FTIR spectra at region of longer wavelengths displays intense and broad peaks at 3032−3674 cm^{-1} , due to stretching vibrations of the −OH/-NH functional groups present on surface. The peaks of less intensity in region of 2800−2940 cm^{-1} belongs to the C−H stretching vibration. The additional peaks of low intensity at ~1635 cm^{-1} and ~1760 cm^{-1} belongs to C=C and C=O functional groups, respectively, the peaks in middle region at 1435 cm−1 can be belongs to C=N stretching vibrations , the peaks corresponds to 1157 and 998 cm^{-1} belongs to P−O/P=O and C−O/C−O−C ; the peak around 550 confirms the presence of PO_4^{3-} *[30-31]*.

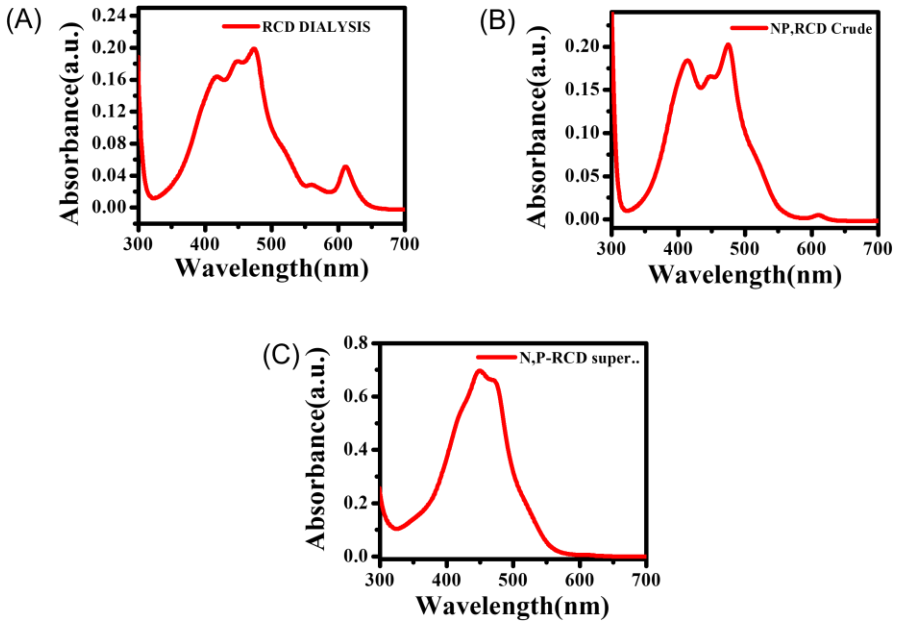

Figure 23. Absorption spectra of (A) dialysed or purified N,P-Carbon dots, (B) crude N,P-Carbon dots and (C) dialysate N,P-Carbon dots.

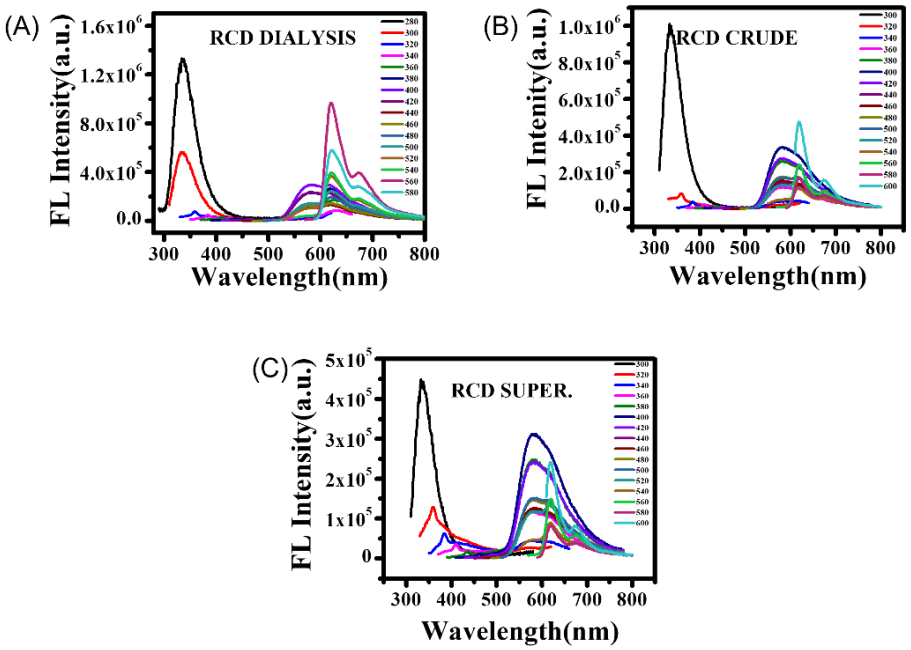

Figure 24. Emission spectra of (A) dialysed or purified N,P-Carbon dots, (B) crude N,P-Carbon dots and (C) dialysate N,P-Carbon dots.

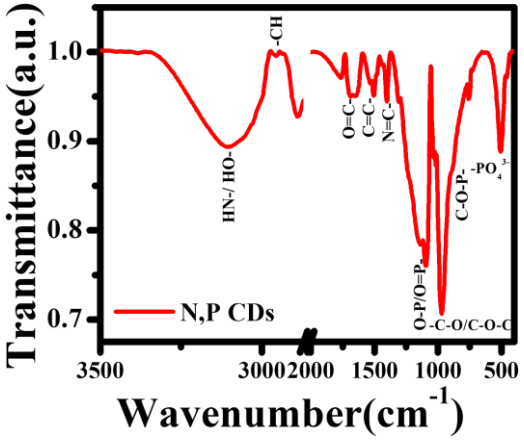

Figure 25 . FTIR spectra of dialysed or purified N,P-Carbon dots.

3.5.2 Characterization of N, P-Carbon dot droplet

The synthesised coacervate droplets were characterised by using UV-vis spectroscopy, fluorescence spectroscopy, and Confocal laser scanning microscopy (CLSM).

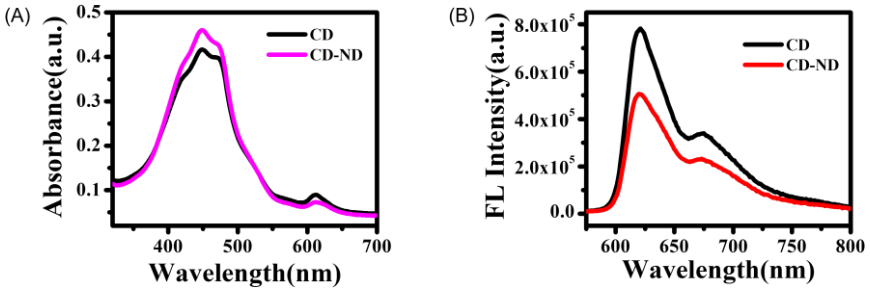

Figure 26. (A) Absorption spectra of N,P-carbon dot and coacervate droplet and (B) Emission spectra of N,P-carbon dot and coacervate droplet.

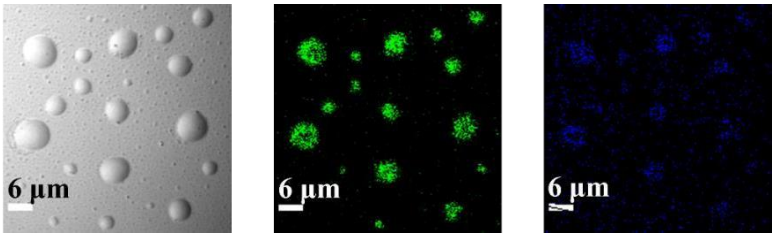

Figure 27 . Confocal images of synthesised N,P-Carbon dot droplet.

3.6 Gold Nanocluster

3.6.1 Characterization of HSA capped gold AuNCs and HSA condensate @AuNCs

The HSA capped gold nanoclusters and HSA condensates @AuNCs were characterised by UV-vis spectroscopy, Fluorescence spectroscopy, CLSM, and FE-SEM. The HSA capped gold nanoclusters show a broad shape absorbance spectra in the UV-Vis spectroscopy (Figure 28A) shows a nanocluster size of less than 3 nm and emission maximum at 670 nm after excitation of 500 nm (Figure 28B). Next, we formed HSA condensates @AuNCs in the presence of 10% PEG 8000 which was confirmed by CLSM images (Figure 28C) and FESEM images (Figure 28D).

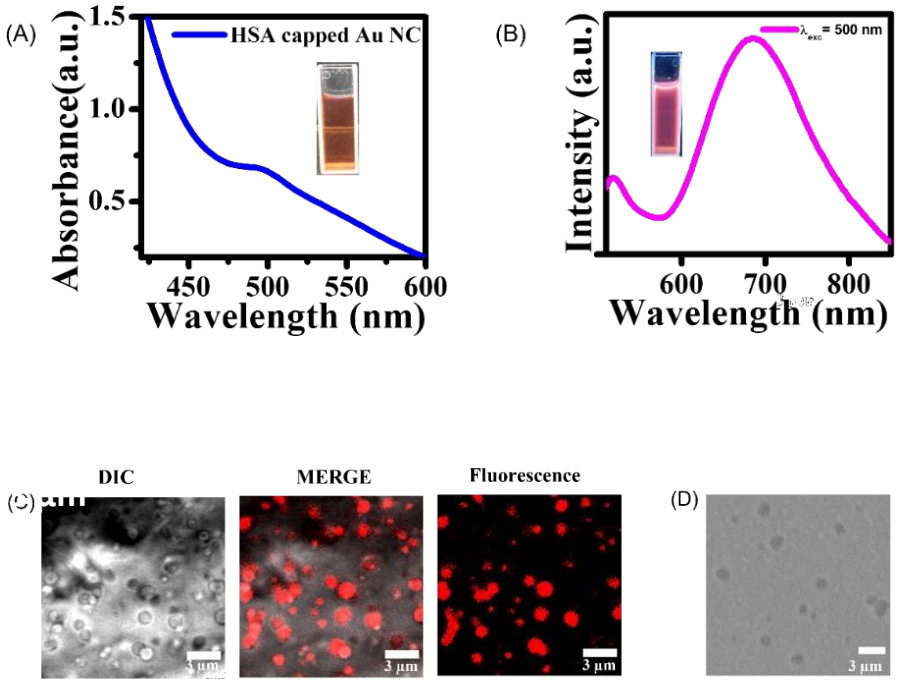

Figure 28. (A) Absorption and (B) fluorescence spectra of HSA capped gold nanoclusters. (C) Confocal and (D) FESEM image of HSA condensates @AuNCs.

CHAPTER 4

Conclusion and Future outlook:

In the present work, we observed that coumarin 480 shows blue shift in its PL spectrum in the presence of SDS micelle. Furthermore, coumarin 480 shows shift in its time-resolved spectra upon entering the stern layer of the micelles. Notably, Coumarin 480 molecules reside in the stern layer of micelles and motion of water molecules is restricted in stern layer and properties of water in stern layer are different those in bulk water.

Next, we successfully fabricated ATP droplets and characterized using CLSM and FESEM imaging. Subsequently coumarin 480 was encapsulated inside the ATP droplets which was further confirmed using CLSM imaging. The encapsulation of coumarin 480 inside the droplets is time dependent i.e., as time increases coumarin 480 loaded inside the droplet shows red shift. The time dependent stokes shift i.e., blue shift of coumarin 480 in ATP droplets and its time-resolved emission spectra shows that intensity decreases with time and small changes in shape of spectrum is invisible because intensity is decreasing with time.

We further fabricated quantum-dot, carbon-dot and nanocluster embedded hybrid droplets which were confirmed using CLSM and FESEM imaging. In future, we will be investigating the behaviour of coumarin 480 inside the carbon dot, quantum dot, and nanoclusters hybrid droplets to understand the behaviour of the interior environment of these hybrid droplets.

REFERENCES

1. Bagchi, B., & Jana, B. (2010), Solvation dynamics in dipolar liquids, Chemical Society Reviews, 39(6), 1936-1954 (DOI: 10.1039/B902048A)
2. Bhattacharyya, K. (2003), Solvation dynamics and proton transfer in supramolecular assemblies, Accounts of chemical research, 36(2), 95-101 (DOI: 10.1021/ar020067m)
3. Sarkar, N., Datta, A., Das, S., & Bhattacharyya, K. (1996), Solvation dynamics of coumarin 480 in micelles, The Journal of Physical Chemistry, 100(38), 15483-15486.
4. Gayen, B., Palchoudhury, S., & Chowdhury, J. (2019), Carbon dots: A mystic star in the world of nanoscience. Journal of Nanomaterials, 2019, 1-19 (DOI: 10.1155/2019/3451307)
5. Saini, B., Singh, R. R., Nayak, D., & Mukherjee, T. K. (2020), Biocompatible pH-responsive luminescent coacervate nanodroplets from carbon dots and poly (diallyldimethylammonium chloride) toward theranostic applications, ACS Applied Nano Materials, 3(6), 5826-5837 (DOI: 10.1021/acsanm.0c00995)
6. Kong, T., Hao, L., Wei, Y., Cai, X., & Zhu, B. (2018), Doxorubicin conjugated carbon dots as a drug delivery system for human breast cancer therapy, Cell proliferation, 51(5), e12488. (DOI: 10.1165/2018/4451907)
7. Ekimov, A. I., & Onushchenko, A. A. (1981), Quantum size effect in three-dimensional microscopic semiconductor crystals, ZhETF Pisma Redaktsiiu, *34*, 363.
8. van de Looij, S. M., Hebels, E. R., Viola, M., Hembury, M., Oliveira, S., & Vermonden, T. (2021), Gold nanoclusters: imaging, therapy, and theranostic roles in biomedical applications, Bioconjugate Chemistry, *33*(1), 4-23.
9. Williams, D. S., Koga, S., Hak, C. R. C., Majrekar, A., Patil, A. J., Perriman, A. W., & Mann, S. (2012), Polymer/nucleotide

droplets as bio-inspired functional micro-compartments, Soft Matter, 8(22), 6004-6014 (DOI: 10.1039/C2SM25184A)

10. Singh, S., Vaishnav, J. K., & Mukherjee, T. K. (2020), Quantum dot-based hybrid coacervate nanodroplets for ultrasensitive detection of Hg^{+2} , ACS Applied Nano Materials, 3(4), 3604-3612 (DOI: 10.1021/acsanm.0c00317)
11. Douliez, J. P., Martin, N., Gaillard, C., Beneyton, T., Baret, J. C., Mann, S., & Beven, L. (2017), Catanionic Coacervate Droplets as a Surfactant-Based Membrane-Free Protocell Model, Angewandte Chemie International Edition, 56(44), 13689-13693 (DOI:10.1002/anie.201707139)
12. Martin, N., Li, M., & Mann, S. (2016), Selective uptake and refolding of globular proteins in coacervate microdroplets. Langmuir, 32(23), 5881-5889 (DOI: 10.1021/acs.langmuir.6b01271)
13. Priftis, D., & Tirrell, M. (2015), Correction: phase behaviour and complex coacervation of aqueous polypeptide solutions, *Soft Matter*, *11*(2), 422-422 (DOI: 10.1039/C4SM90162B)
14. Kim, S., Huang, J., Lee, Y., Dutta, S., Yoo, H. Y., Jung, Y. M., ... & Hwang, D. S. (2016), Complexation and coacervation of like-charged polyelectrolytes inspired by mussels, Proceedings of the National Academy of Sciences, 113(7), E847-E853 (DOI: 10.1073/pnas.1521521113)
15. Vaishnav, J. K., & Mukherjee, T. K. (2019), Highly Photostable and Two-Photon Active Quantum Dot–Polymer Multicolor Hybrid Coacervate Droplets, Langmuir, 35(36), 11764-11773 (DOI: 10.1021/acs.langmuir.9b01783)
16. Strulson, C. A., Molden, R. C., Keating, C. D., & Bevilacqua, P. C. (2012), RNA catalysis through compartmentalization, Nature chemistry, 4(11), 941-946 (DOI: 10.1038/NCHEM.1466)
17. Saini, B., Singh, R. R., Nayak, D., & Mukherjee, T. K. (2020), Biocompatible pH-responsive luminescent coacervate nanodroplets from carbon dots and poly

(diallyldimethylammonium chloride) toward theranostic applications, ACS Applied Nano Materials, 3(6), 5826-5837 (DOI: 10.1021/acsanm.0c00995)

18. Pattni, B. S., Chupin, V. V., & Torchilin, V. P. (2015), New developments in liposomal drug delivery, Chemical reviews, 115(19), 10938-10966 (DOI:10.1021/acs.chemrev.5b00046)
19. Saini, B., Singh, R. R., Nayak, D., & Mukherjee, T. K. (2020), Biocompatible pH-responsive luminescent coacervate nanodroplets from carbon dots and poly (diallyldimethylammonium chloride) toward theranostic applications, ACS Applied Nano Materials, 3(6), 5826-5837 (DOI: 10.1021/acsanm.0c00995)
20. Vaishnav, J. K., & Mukherjee, T. K. (2020), Quantum Dot-Based Hybrid Coacervate Nanodroplets for Ultrasensitive Detection of Hg^{+2} (DOI: 10.1021/acsanm.0c00317)
21. Bhattacharya, A., Chatterjee, S., Prajapati, R., & Mukherjee, T. K. (2015), Size-dependent penetration of carbon dots inside the ferritin nanocages: evidence for the quantum confinement effect in carbon dots, Physical Chemistry Chemical Physics, *17*(19), 12833-12840 (DOI: 10.1039/C5CP00543D)
22. Bhattacharya, A., Chatterjee, S., Khorwal, V., & Mukherjee, T. K. (2016), Luminescence turn-on/off sensing of biological iron by carbon dots in transferrin, Physical Chemistry Chemical Physics, 18(7), 5148-5158. (DOI: 10.1039/C5CP05890B)
23. Bishwal, L., Kar, S., & Bhattacharyya, S. (2023), Role of Noncovalent Interactions in N, P-Functionalized Luminescent Carbon Dots for Ultrasensitive Detection of Moisture in D2O: Boosting Visible-NIR Light Sensitivity, ACS Applied Materials & Interfaces, 15(12), 15907-15916 (DOI: 10.1021/acsami.3c01620)
24. Periaswamy, N., & Kot, A. S. R. (2003), Time resolved fluorescence spectroscopy: TRES and TRANES, Proceedings

of the Indian National Science Academy-Part A: Physical Sciences, 69(1), 41-48 (DOI: 10.1165/1985/3446307)

25. Wang, Z., Long, P., Feng, Y., Qin, C., & Feng, W. (2017), Surface passivation of carbon dots with ethylene glycol and their high sensitivity to Fe^{+3}, RSC advances, 7(5), 2810-2816 (DOI: 10.1039/C6RA25465A).
26. Dong, Y., Li, T., Bateer, B., Wang, H., Fu, Q., & Zhang, F. (2022), Preparation of yellow emissive nitrogen-doped carbon dots from o-phenylenediamine and their application in curcumin sensing, New Journal of Chemistry, 46(20), 9543-9549 (DOI: 10.1039/D2NJ00926A)
27. Dong, Y., Li, T., Bateer, B., Wang, H., Fu, Q., & Zhang, F. (2022), Preparation of yellow emissive nitrogen-doped carbon dots from o-phenylenediamine and their application in curcumin sensing, New Journal of Chemistry, 46(20), 9543-9549 (DOI: 10.1039/D2NJ00926A)
28. Sun, X., Brückner, C., & Lei, Y. (2015), One-pot and ultrafast synthesis of nitrogen and phosphorus co-doped carbon dots possessing bright dual wavelength fluorescence emission, Nanoscale, 7(41), 17278-17282 (DOI: 10.1039/C5NR05549K)
29. Kar, S., Bramhaiah, K., John, N. S., & Bhattacharyya, S. (2021), Insight into the Multistate Emissive N, P-doped Carbon Nano-Onions: Emerging Visible-Light Absorption for Photocatalysis, Chemistry–An Asian Journal, 16(9), 1138-1149 (DOI: 10.1002/asia.202100137)
30. Yu, S. J., Lu, S. Y., Tan, D. F., & Zhu, Y. F. (2022), Nitrogen and phosphorus co-doped carbon dots for developing highly flame-retardant poly (vinyl alcohol) composite films, European Polymer Journal, 164, 110970 (DOI: 10.1016/j.eurpolymj.2021.110970).
31. Mandal, D., Sen, S., Bhattacharyya, K., & Tahara, T. (2002). Femtosecond study of solvation dynamics of DCM in

micelles. Chemical physics letters, 359(1-2), 77-82. (DOI:10.1016/S0009-2614(02)00704-2)